Symmetry breaking in a driven and strongly damped pendulum

Jukka Isohätälä,[1,*] Kirill N. Alekseev,[1,2,†] Lauri T. Kurki,[1] and Pekka Pietiläinen[1]
[1]*Department of Physical Sciences, P. O. Box 3000, University of Oulu FIN-90014, Finland*
[2]*Theory of Nonlinear Processes Laboratory, Kirensky Institute of Physics, Krasnoyarsk 660036, Russia*
(Received 13 October 2004; revised manuscript received 15 March 2005; published 15 June 2005)

We examine the conditions for appearance of a symmetry breaking bifurcation in damped and periodically driven pendulums in the case of strong damping. We show that symmetry breaking, unlike other nonlinear phenomena, can exist at high dissipation. We prove that symmetry breaking phases exist between phases of symmetric normal and symmetric inverted oscillations. We find that symmetry broken solutions occupy a smaller region of the pendulum's parameter space in comparison to the statements made in earlier considerations [McDonald and Plischke, Phys. Rev. B **27**, 201 (1983)]. Our research on symmetry breaking in a strongly damped pendulum is relevant to an understanding of the phenomena of dynamic symmetry breaking and rectification in pure ac driven semiconductor superlattices.

DOI: 10.1103/PhysRevE.71.066206 PACS number(s): 05.45.−a, 02.30.Oz, 73.21.Cd, 74.50.+r

I. INTRODUCTION

Periodically forced and damped pendulum

$$\ddot{\theta} + \gamma\dot{\theta} + \sin\theta = f\cos\omega t \tag{1}$$

is one of the most important paradigms in modern nonlinear science [1]. In solid state physics, the pendulum model well describes, for instance, the nonlinear dynamics of Josephson junctions of superconducting materials [2,3].

The fairly popular model of a resistively shunted Josephson junction [4,5] which is equivalent to an underdamped pendulum, $\gamma \ll 1$, demonstrates very rich nonlinear dynamics. The rotational states of the pendulum $\langle\dot{\theta}\rangle \neq 0$ (averaging over a period $T=2\pi/\omega$), correspond to the generation of a dc voltage across the junction driven by an ac current without a dc component. Moreover, phase-locked states of the pendulum, $\langle\dot{\theta}\rangle = n/m$ (n and m are integers), correspond to quantized values of the dc voltage in the Josephson junction model. This effect, known as the inverse ac Josephson effect [6,7], has already found an application in the design of the modern voltage standard [3,8]. Chaotic vibrational and rotational motions of an underdamped pendulum, $\gamma \ll 1$, are also well known in Josephson junctions [9,10] (for a review see [11]). Surprisingly, the optimum operating point for the voltage standards in (ω, f) parameter space is located near a region of chaos [3]. Therefore, knowledge of conditions for transition to chaos is important for the optimization of a zero-bias voltage standard and related Josephson devices [3,8].

One of the most often observed roads to chaos is the period doubling scenario [12]. The pendulum (1) belongs to a class of symmetric dynamical systems with invariance under the transformations $\theta \to -\theta$ and $t \to t+T/2$. Therefore, a symmetry breaking bifurcation is a necessary precursor to period doubling [10,13,14]. This bifurcation describes a sharp transition from a symmetric limit cycle satisfying

$$\theta(t+T/2) = -\theta(t) + 2\pi k, \quad k \text{ is an integer}, \tag{2}$$

to symmetry broken limit cycles, for which this equality is invalid. As easily seen from Eq. (1), steady-state symmetric solutions $\theta(t)$ can have only odd harmonics of ω in their Fourier expansion series, together with a zero harmonic $\langle\theta\rangle$ that is equal to either 0 or π. The solutions with $\langle\theta\rangle = 0$ are symmetric oscillations around the stable position $\theta = 0$, while $\langle\theta\rangle = \pi$ corresponds to oscillations of an inverted pendulum. In contrast, for symmetry broken solutions both even and odd harmonics are possible and $\langle\theta\rangle$ is some constant different from 0 or π. Typically, the symmetry broken trajectories of the underdamped pendulum occupy a very small range of parameters ωf just near the transition to chaos [10,13,15]. A detailed analytical analysis of a transition from symmetric oscillations to symmetry broken oscillations near the chaos border in the underdamped pendulum, $\gamma \ll 1$ and $\omega < 1$, is presented in [16]. A different, more mathematically oriented, approach to the bifurcations of symmetric solutions of Eq. (1) with a general antiperiodic drive term can be found in [17].

In spite of a widely spread belief that symmetry breaking is always connected to a transition to chaos [14], this bifurcation is still possible for $\gamma \ll 1$ but $\omega > 1$ [18]. In these conditions chaos is impossible and symmetry breaking arises near transitions from normal to inverted states of the pendulum [18].

For a strong damping ($\gamma \gtrsim 1$), neither chaotic [19,20] nor rotational phase-locked states [10] can exist anymore. However, the presence of symmetry broken states of an overdamped pendulum, which obviously are not related to a transition to chaos, has been briefly mentioned earlier in two papers devoted to the dynamics of Josephson junctions [13,21]. It has been reported [13] that these symmetry broken trajectories occupy a quite large part of the parameter space (ω, f). This interesting aspect of the pendulum dynamics at strong dissipation did not get further attention so far, probably for two main reasons. First, for Josephson junctions, the

*Electronic address: jisohata@student.oulu.fi
†Electronic address: Kirill.Alekseev@oulu.fi

pendulum's solutions at strong damping are not physically interesting. Second, θ and $\langle\theta\rangle$ do not correspond to any directly measurable physical variables in the junctions.

However, it has been shown recently that another type of solid state microstructure—semiconductor superlattices subjected to a high-frequency electric field—can demonstrate very rich nonlinear dynamics similar to the dynamics of Josephson junctions [22–27]. In particular, an analog of the inverse ac Josephson effect has been predicted for the superlattices [23,25]. Moreover, within some reasonable approximations the nonlinear dynamics of an ac driven semiconductor superlattice in the miniband transport regime is governed by a periodically forced and damped pendulum [26,27]. For superlattices with realistic scattering constant [28,29], the effective damping in the corresponding pendulum model is not small: $\gamma \gtrsim 1$. An overdamped pendulum also arises in the models of lateral semiconductor superlattices [30].

Importantly, in contrast to the case of Josephson junctions, the voltage across a superlattice is proportional to both the velocity $\dot{\theta}$ and the coordinate θ of the pendulum (1) [26]. Therefore, even if rotations are impossible, $\langle\dot{\theta}\rangle \neq 0$, a dc voltage across the superlattice can still be generated due to contributions of symmetry broken swinging oscillations with $\langle\theta\rangle \neq l\pi$ $(l=0,1)$. For a strong damping, this is the only mechanism that can contribute to a rectification of the terahertz signal in the semiconductor superlattice [26].

The existence of physical situations where the symmetry breaking in the pendulum at strong dissipation can be physically important is the main motivation of our present work. Combining the analytical technique of truncated Fourier expansion [31] with numerical simulations we find the conditions for symmetry breaking at strong damping. We describe a scenario of transition from symmetric to asymmetric oscillations at strong damping. We found that symmetry broken (SB) oscillations form an intermediate stage between symmetric normal (N) and symmetric inverted (I) oscillations, i.e., $N \rightarrow \mathrm{SB} \rightarrow I \rightarrow \mathrm{SB} \rightarrow N$. Note that this is different from the transitions $N \rightarrow \mathrm{SB} \rightarrow N$ with a large symmetry breaking phase even in the overdamped case, which have been reported in [13]. We observed a relatively small symmetry breaking phase; with an increase of damping the ranges of driving amplitude and frequency resulting in symmetry breaking decrease. Moreover, symmetry breaking does not exist in the overdamped case described by the first order differential equation. In this case only normal and inverted oscillations survive. We presented simple formulas providing a good approximation for bifurcation points between different types of symmetric $(N \rightarrow I)$ and asymmetric $(N \rightarrow \mathrm{SB}, I \rightarrow \mathrm{SB})$ transitions in wide ranges of the frequency and the strength of alternating force.

The organization of this paper is as follows. We start with a consideration of an overdamped pendulum without an inertial term $(\ddot{\theta}=0)$. The analysis of this model appears to be the most simple and transparent. In the subsequent Section III, we present analytic and numerical results on symmetry breaking bifurcations in a pendulum with an inertial term. The final section of the paper is devoted to a summary and a brief discussion on applications in the physics of semiconductors. Some mathematical details that have been omitted can be found in [32].

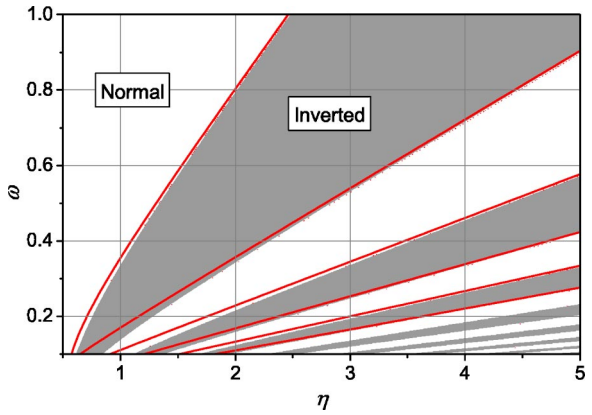

FIG. 1. (Color online) First order pendulum, with $\beta=1/2$: regions of inverted and normal mode oscillations. White areas correspond to normal oscillations with $\langle\theta\rangle=0$ and gray areas to the inverted mode $\langle\theta\rangle=\pi$. No symmetry broken solutions are found. Solid (red) lines indicate the analytic prediction for mode boundaries, Eq. (8), which are plotted for $n=1,\ldots,6$.

II. FIRST ORDER PENDULUM EQUATION

When damping is very strong we can neglect the second order derivative in Eq. (1) and get the first order overdamped pendulum equation

$$\dot{\theta} + \beta \sin\theta = \eta \cos\omega t \tag{3}$$

with $\beta=1/\gamma$ and $\eta=f/\gamma$. Numerical integration of this equation shows that only two types of stable periodic motion exist: normal and inverted modes of oscillations. Solutions corresponding to these modes are all symmetric with $\langle\theta\rangle=0$ and π for the normal and inverted mode solutions, respectively. Figure 1 shows a plot of regions of the two different modes in the (f,ω) parameter plane which exhibits a fan shaped pattern of alternating, disjoint areas of normal and inverted mode oscillations. The transition between the two modes is a sharp one and no intermittent states are found in spite of rigorous attempts. In particular, no symmetry broken regions exist.

A simple analytic calculation verifies the absence of symmetry broken solutions and provides a good approximate condition for the transition. The analysis is done under the assumption that the solution is well described by the trial function

$$\theta = A_0 + A_1 \cos(\omega t + \alpha_1). \tag{4}$$

We begin by applying a linear stability analysis to find the regions of stable symmetric motion. Straightforward analysis leads to the stability condition

$$\beta \cos A_0 J_0(A_1) > 0, \tag{5}$$

where J_0 is the zeroth order Bessel function. If for the zeroth harmonic we have $\cos A_0 < 0$, then $J_0(A_1) > 0$ must apply, and vice versa. Both symmetric solutions lose their stability at the same A_1, which is a root of the Bessel function J_0. As the Bessel functions and the zeros of J_0 will appear frequently, we adopt the shorthand notations

$$J_0(A^{(n)}) = 0, \quad J_k^{(n)} \equiv J_k(A^{(n)}), \tag{6}$$

where $A^{(n)}$ is specifically the nth root of J_0 and $J_k^{(n)}$ is J_k evaluated at $A^{(n)}$.

From the equation of motion, Eq. (3), we can derive using the ansatz (4) the relation

$$J_0(A_1)\sin A_0 = 0. \tag{7}$$

From Eq. (7) it follows that if $A_0 \neq 0, \pi$, then $J_0(A_1)=0$. However, the stability condition (5) indicates that this case is not stable, as the perturbation does not decay. Therefore it is evident that asymmetric trajectories are not possible.

Within the applicability of our first order approximation, the only stable solutions are the ones with $A_0=0$ or π. Additionally, the pattern of normal and inverted mode solutions is revealed. Starting from a forcing η low enough, i.e., one for which $J_0(A_1)>0$, Eq. (5) implies that $A_0=0$. When A_1 crosses $A^{(1)}$, the sign must change in both factors, leading to $A_0=\pi$. As η is further increased, A_1 reaches $A^{(2)}$ and the oscillations return to the normal mode.

The boundaries of the normal and inverted oscillations can even be written in an explicit analytic form. From Eq. (3) the expansion coefficient A_1 in Eq. (4) can be found as a function of the pendulum parameters. Substituting $A_1=A^{(n)}$ we get

$$4\beta^2 J_1^{(n)2} + \omega^2 A^{(n)2} = \eta^2. \tag{8}$$

Now we can compare our analytic results with numerical data. The boundaries of transitions between normal and inverted modes of oscillation, following from Eq. (8), are superimposed on the numerical results in Fig. 1. We see that the the equality $J_0(A_1)=0$ and the prediction of Eq. (8) hold well at the transition lines with reasonable accuracy everywhere, except in the case of low frequency. In the limiting case of very low-frequency drive, the trial solution in the simplest form (4) can become invalid and effects of higher harmonics should be taken into account.

III. SYMMETRY BREAKING IN THE PENDULUM AT STRONG DISSIPATION

A. Numerical integration

Now we return to the pendulum with inertia, Eq. (1). We start with a review of our numerical results. For all computations, standard double precision floating point arithmetic has been used. Numerical integration was performed using a standard 4/5 order Runge-Kutta algorithm with Cash-Karp parameters [33].

The study of the (ω, f) parameter plane reveals a fan shaped structure of regions of normal and inverted mode oscillations, similar to that of the first order pendulum. In addition to the alternating pattern of the symmetric solutions, narrow regions of symmetry broken solutions have now emerged on the interfaces between the regions. For the solutions in these regions we have observed nonzero values of the zero-harmonic components along with nonzero even harmonics, which are requisites of a symmetry broken solution.

In Fig. 2 an example of a typical phase-space portrait is plotted. Therein, both solutions θ_1 and θ_2, which are related via the symmetry $\theta_1(t)=-\theta_2(t+T/2)$, are shown. For these symmetric solutions the orbits are centered around an integer multiple of π and can either overlap or be separated by a multiple of 2π. This is shown in the insets on the right, where orbits just before and after the symmetry breaking region are plotted. In the lower right corner, $f=4.50$, an inverted mode solution is depicted. The oscillations are centered around $\pm\pi$ and the orbits are separated by 2π, making them in fact one and the same. For forcing of $f=4.65$ the asymmetry of the orbit is clearly visible as well as the shifted center of the oscillations. Finally, at $f=4.80$, the solution is symmetric again with the two orbits now overlapping, shown on the upper right inset.

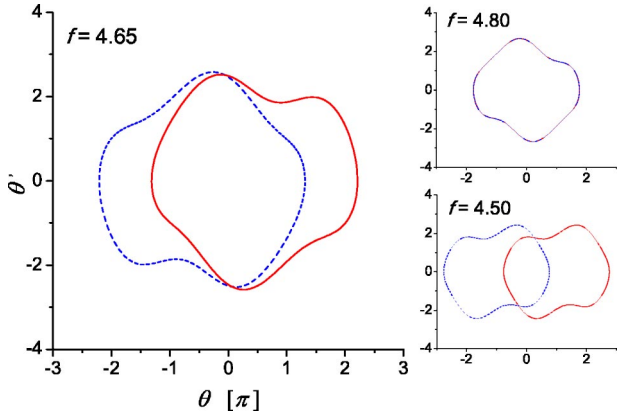

FIG. 2. (Color online) Phase-space portrait of a typical symmetry broken solution. To highlight the asymmetry both solutions θ_1 [solid (red)] and θ_2 [dashed (blue)], which are related via the symmetry $\theta_1(t)=-\theta_2(t+T/2)$, are plotted. Taking f as the control parameter, the insets on the right show the orbit just before and after the symmetry breaking. This is the $n=2$ transition; therefore it is from inverted to normal mode. The fixed parameters are $\gamma=2$ and $\omega=0.4$.

The different modes on the parameter plane are depicted in Fig. 3, where we have chosen $\gamma=2$ for the damping coefficient. Symmetry broken regions appear around both transitions, from normal to inverted and back, thus separating the normal and inverted mode regions completely. The regions

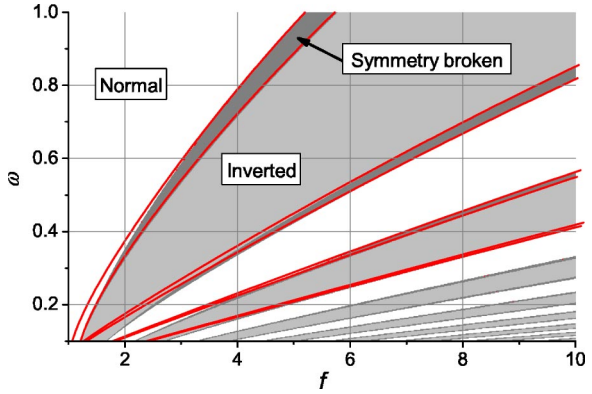

FIG. 3. (Color online) Second order pendulum equation with $\gamma=2$: regions of inverted and normal state oscillations. Sandwiched between them are the regions of symmetry breaking. Solid (red) lines indicate analytic prediction of Eqs. (12) and (10).

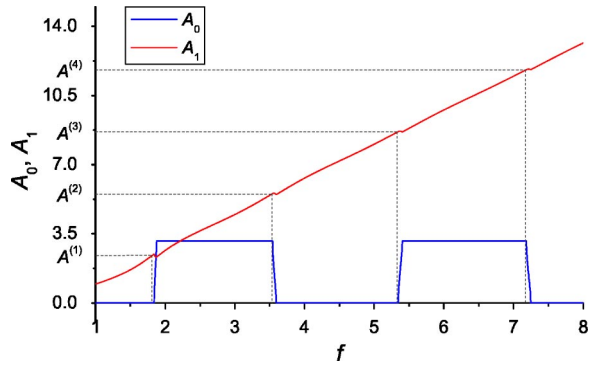

FIG. 4. (Color online) The amplitudes of the two first harmonic components A_0 and A_1 plotted against f. A_0 [lower curve (blue)] alternates between *0* and π, while A_1 [upper curve (red)] shows nearly linear dependence on the parameter f. Small deviations from this are seen near the transitions between normal and inverted states, along with an A_0 component that is not equal to 0, π. To guide the eye, dashed lines connecting the points $A_1(f)=A^{(n)}$ on the vertical axis to the corresponding f on the horizontal axis are drawn. The fixed pendulum parameters are $\gamma=3$ and $\omega=0.2$.

are not wide, in contrast to what was reported in [13,34]. Increasing the damping will cause them to get more narrow.

A closer examination is shown in Fig. 4, where we have fixed $\omega=0.2$ and $\gamma=3$. Harmonic components A_0 and A_1 are plotted against the drive amplitude f, and the sequence of modes of solutions is made more clear. The normal mode bifurcates into asymmetric solutions when A_1 is close to a root of the Bessel function $J_0(A_1)$. This symmetry broken state persists only for a short interval of variable f, ending in an inverted mode, when A_0 has reached π. Small deviations from an approximately linear response of A_1 to a change of f can be seen at the transitions from normal to inverted mode.

Close-ups of the symmetry broken range provide more insight. The following two examples are depicted in Fig. 5. The first case we consider is of low-frequency drive, $\omega=0.2$ and $\gamma=3$. Symmetry breaking starts for moderate forcing $f=1.8413$ and with A_1 slightly larger than $A^{(1)}$, the first root of J_0. The curve of A_0 for the stable symmetric solution bifurcates from zero into a curve corresponding to a stable asymmetric solution. This is accompanied by the emergence of even harmonics in the Fourier spectrum and a sudden stop in the increase of A_1. Further increases of f cause A_1 to decrease, while A_2 traces a sugar-loaf-shaped curve. It should be noted that the curve of the second harmonic reaches quite high values, $A_2\sim 0.6$ at the maximum. The zero harmonic varies continuously and monotonically from zero to π. We should note that actually two different stable solutions exist in the symmetry breaking range, related to each other by the symmetry. The initial values of the system determine which branch the solution converges to after the initial transient. Symmetry breaking ends in an inverted state at $f=1.8773$ with A_1 just less than $A^{(1)}$.

In the second case we examine, we set $\omega=4$ and $\gamma=3$. To achieve symmetry breaking, one needs high values of f. In this case we have $f=47.46$. Again, A_1 has just crossed $A^{(1)}$ when the symmetric mode loses stability. Now the decrease of A_1 in the symmetry broken region is less dramatic than in the low-frequency case. Furthermore, the second harmonic component is almost negligible. In other respects, this case does not differ from the previous example.

B. Analytic analysis

In this subsection we present the explicit analytic form of conditions for the bifurcation to occur and provide a picture of the scenario of symmetry breaking that is consistent with the numerical results. Here, as in Sec. II, we assume that oscillations of the pendulum can be described by a trial function in the form (4).

Following the method of [10,31], we linearize Eq. (1) and, with appropriate approximations, put it into the form of the Mathieu equation. Using the existing knowledge of the solutions of Mathieu equation, we derive the following conditions for bifurcations from symmetric oscillations:

$$J_0(A_1) + (-1)^k \frac{2}{\gamma^2 + 4\omega^2} J_2(A_1)^2 = 0, \tag{9}$$

where $k=0$ corresponds to a normal mode, while $k=1$ marks an inverted mode. Notice that Eq. (9) is the same condition for loss of stability as the one for the first order pendulum, $J_0(A_1)=0$, but now with an additional term. This term only becomes significant when A_1 is close to a root of the Bessel function J_0. As a consequence, now there are two separate bifurcation points corresponding to the two different symmetric modes. These are located rather close to the roots of J_0. Clearly, the dynamics of the second and the first order pendulums are similar away from the regions of transition, justifying the correspondence to the analysis of the previous section.

The explicit solution of Eq. (9) in terms of amplitude A_1 can now be found. Owing to the fact that the latter term in Eq. (9) is small, we get for the critical values of A_1

$$\left.\begin{matrix} A_N^{(n)} \\ A_I^{(n)} \end{matrix}\right\} = A^{(n)} \pm \frac{2J_2^{(n)2}}{J_1^{(n)}(\gamma^2 + 4\omega^2) \mp \chi^{(n)}}, \tag{10}$$

$$\chi^{(n)} = 2J_2^{(n)}(J_1^{(n)} - J_3^{(n)}). \tag{11}$$

Here $A_N^{(n)}$ and $A_I^{(n)}$ are, respectively, the critical amplitudes of normal and inverted modes for which symmetric oscillations become unstable. A small asymmetry with respect to $A^{(n)}$ in the critical A_1 due to the term $\chi^{(n)}$ can be neglected within the applicability of Eq. (10) without loss of qualitative agreement. This is implicitly assumed hereafter in this section.

In transitions from the normal to the next inverted mode, the critical value of the amplitude A_1 for the inverted mode is less than that of the normal mode: $A_I^{(n)}<A_N^{(n)}$. The reverse applies for transitions from an inverted phase to the next normal phase region, i.e., $A_N^{(n)}<A_I^{(n)}$. Therefore A_1 must decrease as the boundary of the first symmetry broken region is crossed, and the nth region starts when $A_1>A^{(n)}$ and ends when $A_1<A^{(n)}$. This kind of behavior of A_1 is in good agreement with the numerical results shown in Fig. 5. Following Eq. (10) the difference between $A_N^{(n)}$ and $A_I^{(n)}$ decreases with an increase of the frequency ω. This explains why the range of A_1 within the symmetry breaking region is wider in the

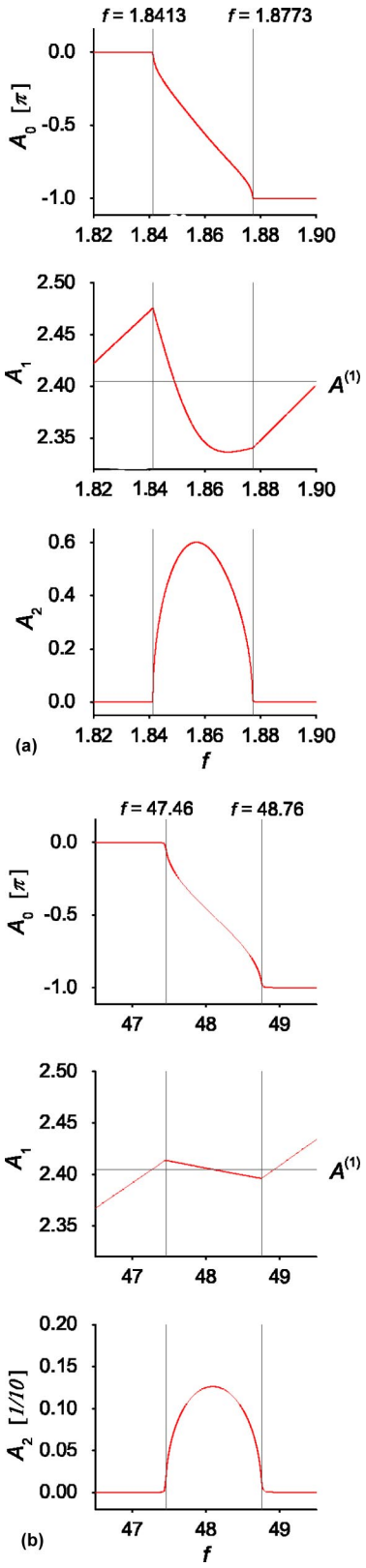

FIG. 5. (Color online) The amplitudes of the two first harmonic components as functions of the drive amplitude f. (a) Low frequency and weak drive, $\gamma=3$ and $\omega=0.2$; (b) high frequency and strong drive, $\gamma=3$ and $\omega=4$. Notice the relatively large amplitude of the second harmonic component in the low-frequency case.

low-frequency case in comparison with the case of high-frequency drive [see Figs. 5(a) and 5(b)].

We turn now to finding surfaces in the parameter space (γ,ω,f) on which the symmetry breaking bifurcation happens. First, we substitute the trial solution (4) in the equation of motion (1) and in the first harmonic approximation derive the dependence of the amplitude A_1 on the pendulum parameters γ, ω, and f. Second, substituting critical values of A_1 from Eq. (10) and taking $A_0=k\pi$, we have

$$f^2=(\gamma\omega A_1)^2+[\omega^2A_1\pm 2J_1(A_1)]^2,\quad \begin{cases} A_1=A_I^{(n)}, \\ A_1=A_N^{(n)}, \end{cases} \tag{12}$$

for bifurcations from inverted and normal modes, respectively. Taking the difference of these two critical f does indicate that one symmetric mode loses stability before the other gains it. This eliminates the possibility of hysteresis around the symmetry breaking transition and shows that both symmetric phases cannot be stable for the same pendulum parameters.

Equation (12) shows remarkable agreement with our numerical results for a very wide range of parameters. As an example we refer to Fig. 3, where the analytic predictions for the boundaries of symmetry breaking regions are shown as solid (red) lines. The best agreement is achieved for $\omega\gtrsim 1$ or large f. These conditions also provide the applicability of our trial function (4), which has been proved numerically as well as analytically by including the third harmonic into the trial function [32]. We should also note that good qualitative agreement between our formulas and numerical results exists even for low frequencies, $\omega\simeq 0.1$. Moreover, our analytic results give a reasonable approximation even in parameter space regimes beyond the overdamped case, providing f is sufficiently large and ω is not very low. This suggests that as the damping or frequency is lowered from sufficiently high values, the symmetry broken regions evolve into regions of complex and chaotic dynamics with alternating normal and inverted phase motion separating them.

Now we can summarize the main results of the present section. Taking the alternating force strength f as the control parameter, we can report the following behavior. A stable inverted or normal mode becomes unstable at an amplitude of stationary oscillations, A_1, that is just greater than $A^{(n)}$ and symmetry breaking starts. Increasing f further causes A_1 to decrease, as the bifurcation to the next mode should occur when A_1 is less than $A^{(n)}$. The critical values of A_1 are given by Eq. (10) with the critical parameters of Eq. (12). These critical points approach a common value $A^{(n)}$, as damping is increased.

IV. CONCLUSION

In summary, we confirmed the existence of the symmetry breaking phenomenon in the strongly damped pendulum. The symmetry breaking states form a necessary stage in transitions from the normal to the inverted and from the inverted to the normal states of the overdamped pendulum. The scenario of transitions from the symmetric to the symmetry broken states, and vice versa, appears to be similar to the case of

the underdamped pendulum without chaos [18]. Also, our results compare well to those of [17]. Therein the sufficient conditions for the symmetric solutions to be the only periodic solutions were derived and it was shown that the stability of the symmetric solutions alternates between the regions where the given requirements do not hold.

Our results also demonstrate that an inertial term in the pendulum is a requisite of symmetry breaking. On a more hypothetical note, it could then be possible to achieve symmetry breaking similar to what is described here, if higher even derivatives or/and additional nonlinear damping terms are included.

These results can be directly applied to studies of the mechanism of terahertz radiation rectification in semiconductor superlattices [25] because this system has underlying pendulum dynamics [26,30]. Note that in some cases a pendulumlike equation of the third order [35,36] and a pendulum equation with a nonlinear damping term supporting the symmetry of the problem [37] naturally arise in different models of semiconductor superlattices. We speculate that swinging symmetry broken oscillations in these superlattice models also correspond to spontaneous generation of a dc voltage or dc current. A related detailed consideration will be published elsewhere. It is worth noticing also the importance of the symmetry breaking bifurcations in the physics of ac driven bulk semiconductors with different types of nonlinearity [38]. Our results can also be useful in the development of this area of semiconductor nonlinear dynamics.

ACKNOWLEDGMENTS

We thank G. Katriel for attracting our attention to Ref. [17]. This research was partially supported by the Academy of Finland (Grants No. 1206063 and No. 100487) and the AQDJJ Program of the European Science Foundation.

[1] R. Z. Sagdeev, D. A. Usikov, and G. M. Zaslavsky, *Nonlinear Physics: From the Pendulum to Turbulence and Chaos* (Harwood Academic Publishers, Chur, Switzerland, 1992).
[2] K. Likharev, *Dynamics of Josephson Junctions and Circuits* (Gordon and Breach, New York, 1986).
[3] R. L. Kautz, Rep. Prog. Phys. **59**, 935 (1996).
[4] D. E. McCumber, J. Appl. Phys. **39**, 3113 (1968).
[5] W. C. Stewart, Appl. Phys. Lett. **12**, 277 (1968).
[6] D. N. Langenberg, D. J. Scalapino, B. N. Taylor, and R. E. Eck, Phys. Lett. **20**, 563 (1966).
[7] M. T. Levinsen, R. Y. Chiao, M. J. Feldman, and B. A. Tucker, Appl. Phys. Lett. **31**, 776 (1977).
[8] C. A. Hamilton, Rev. Sci. Instrum. **71**, 3611 (2000).
[9] B. A. Huberman, J. P. Crutchfield, and N. H. Packard, Appl. Phys. Lett. **37**, 750 (1980).
[10] D. D'Humieres, M. R. Beasley, B. A. Huberman, and A. Libchaber, Phys. Rev. A **26**, 3483 (1982).
[11] U. Krüger, J. Kurkijärvi, M. Bauer, and W. Martienssen, in *Nonlinear Dynamics in Solids*, edited by H. Thomas (Springer-Verlag, Berlin, 1992).
[12] J.-P. Eckmann, Rev. Mod. Phys. **53**, 643 (1981).
[13] A. H. MacDonald and M. Plischke, Phys. Rev. B **27**, 201 (1983).
[14] J. W. Swift and K. Wiesenfeld, Phys. Rev. Lett. **52**, 705 (1984).
[15] W. C. Kerr, M. B. Williams, A. R. Bishop, K. Fesesr, P. S. Lomdahl, and S. E. Trullinger, Z. Phys. B: Condens. Matter **59**, 103 (1985).
[16] J. Miles, Physica D **31**, 252 (1988).
[17] G. Katriel, J. Diff. Eqns. **182**, 1 (2002).
[18] N. Takimoto and M. Tange, Prog. Theor. Phys. **90**, 817 (1993).
[19] M. Levi, Phys. Rev. A **37**, 927 (1988).
[20] T. H. Yang, C. S. Wang, J. C. Huang, and Y. S. Gou, Phys. Rev. E **51**, 5279 (1995).
[21] M. Octavio, Phys. Rev. B **29**, 1231 (1984).
[22] D. H. Dunlap, V. Kovanis, R. V. Duncan, and J. Simmons, Phys. Rev. B **48**, 7975 (1993).
[23] A. A. Ignatov, E. Schomburg, J. Grenzer, K. F. Renk, and E. P. Dodin, Z. Phys. B: Condens. Matter **98**, 187 (1995).
[24] K. N. Alekseev, G. P. Berman, D. K. Campbell, E. H. Cannon, and M. C. Cargo, Phys. Rev. B **54**, 10625 (1996).
[25] K. N. Alekseev, E. H. Cannon, J. C. McKinney, F. V. Kusmartsev, and D. K. Campbell, Phys. Rev. Lett. **80**, 2669 (1998).
[26] E. H. Cannon, F. V. Kusmartsev, and D. K. Campbell, Europhys. Lett. **56**, 842 (2001).
[27] K. N. Alekseev and F. V. Kusmartsev, Phys. Lett. A **305**, 281 (2002).
[28] K. Unterrainer, B. J. Keay, M. C. Wanke, and S. J. Allen, Phys. Rev. Lett. **76**, 2973 (1996).
[29] S. Winnerl *et al.*, Phys. Rev. B **56**, 10303 (1997).
[30] K. N. Alekseev *et al.*, Europhys. Lett. **70**, 292 (2005).
[31] N. F. Pedersen, O. H. Soerensen, B. Dueholm, and J. Mygind, J. Low Temp. Phys. **38**, 1 (1980).
[32] J. Isohätälä, K. N. Alekseev, L. T. Kurki, and P. Pietiläinen, e-print cond-mat/0409572.
[33] J. R. Cash and A. H. Karp, ACM Trans. Math. Softw. **16**, 201 (1990).
[34] The pattern of symmetric inverted oscillations plus the nearest symmetry breaking region in our computations is found to be quite similar to the pattern described as "symmetry broken" for the overdamped pendulum in Ref. [13]. This might be explained by observing that technique used in [13] to detect symmetry broken trajectories at strong damping cannot in fact distinguish between symmetric inverted and instant asymmetric solutions.
[35] A. P. Tetervov, Izv. Vyssh. Uchebn. Zaved., Radiofiz. **27**, 801 (1984) [Radiophys. Quantum Electron. **27**, 564 (1984)].
[36] F. G. Bass and A. P. Tetervov, Phys. Rep. **140**, 237 (1986).
[37] K. N. Alekseev and A. Malkin (unpublished).
[38] S. Bumyalene, G. Lasene, and K. Piragas, Fiz. Tekh. Poluprovodn. (S.-Peterburg) **23**, 1479 (1989) [Sov. Phys. Semicond. **23**, 918 (1989)].